

## THE MEASUREMENT OF HEAT FLOW WITHIN A DC CASTING MOULD

A. Prasad<sup>1</sup>, J.A. Taylor<sup>1</sup>, I.F. Bainbridge<sup>1</sup>.

<sup>1</sup>CAST CRC, University of Queensland, Brisbane, QLD 4072, Australia

Keywords: DC casting, Mould-wall, Heat Flow

### Abstract

The heat flow between the molten metal and the mould-wall in DC casting is often assumed to be negligible compared to that due to the sub-mould water cooling. Furthermore, the entire DC casting process is often described based on this assumption. However, the assumption of negligible heat transfer in the metal-mould region, as compared to the sub-mould region, and its subsequent minimal influence on cast product quality remains unproven. The focus of the present paper is therefore on understanding the heat transfer in the metal/mould wall region. To this end a method for the laboratory measurement of the flow of heat from the metal being cast to the wall of a DC casting mould has been developed. The equipment and methodology are briefly described together with some of the initial results obtained. The implications of this work for use in simulation models and for the design and operation of DC casting moulds are discussed.

### Introduction

The practice of DC casting of aluminium and aluminium alloys requires the removal of heat from the surface of the solidifying metal at two points within the system: the sub-mould cooling impingement area (often referred to as the primary cooling zone) and the mould wall area. Heat flow in the sub-mould cooling area has been reasonably well studied and confirmed values are available for the heat transfer coefficient for a range of casting conditions [1-4]. Several estimates of the mould wall heat transfer have been made, together with some attempts to measure the heat flow during an actual cast. Table 1 summarises the current data available.

Knowledge of the actual heat flow from metal to the mould wall and the factors that influence this are thought to be important for both the design and operation of a DC casting mould [5, 6]. In fact, cast product quality has been directly linked to the amount of heat removed through the mould wall [7, 8]. Moreover, accurate simulation of the process by mathematical modelling is dependent upon reliable data for this factor.

The measurement of the mould wall heat flow under controlled conditions during an actual DC cast is extremely difficult and costly. Determination of the effect of individual factors that may have an influence on the mould wall heat flow is not possible under such conditions. The objective of the work reported in the paper was to develop a laboratory simulation of an operating mould and to use this to accurately measure the heat transfer coefficient between the molten metal and the simulated mould wall under a range of controlled conditions known to occur within a DC casting mould. A description of the equipment and experimental methodology developed is given, together with the important factors that have been found to influence the results. A

comparison of these results with those shown in Table 1 is made and reasons for the differences are suggested. Finally mention is made of the possible use of the results for process refinement.

Table 1. Published values for mould wall heat flow

Parameter	Value	Units	Ref.
Heat transfer coefficient – molten metal to mould	2000	W/m <sup>2</sup> /K	[9]
	3000		[10]
	2400		[11]
	1000		[7]
	1000–2000		[12]
Heat transfer coefficient – air gap formed in mould	200	W/m <sup>2</sup> /K	[9]
	250 – 350		[10]
Heat flux – molten metal to mould wall – <i>Hot top casting</i> <i>Air pressurized casting</i> <i>Rolling block casting – Sumitomo</i>	1270 420 ~800	kW/m <sup>2</sup>	[7]
			[7]
			[14]
			[14]
Rate of heat removal through the mould (for 152mm dia. 6063 billet cast at 101, 152 & 228 mm/min.)	7,600	W (% of total)	[15]
	(9.1%)		
	11,000		
	(9.0%)		
	18,000		
(10.4%)			

### Basic concepts

Figure 1 shows a schematic of liquid metal solidifying within the mould wall region of a DC casting. The concepts involved in the measurement of the metal/mould wall gap heat transfer coefficient ( $h_g$ ) for a DC casting mould are relatively simple and involve the determination of the two temperature differences ( $\Delta T_1$  and  $\Delta T_2$ ) and the two distances ( $L_1$  and  $L_2$ ). Note that the schematic in Figure 1 is not to scale. The gap between the mould-wall and the liquid-metal ( $L_1$  in the figure) in an actual casting is significantly smaller than the mould-wall thickness ( $L_2$ ).

Knowing the temperature difference ( $\Delta T_2$ ) across the mould section (from the front casting face to the water cooled rear section, i.e. distance  $L_2$ ) and the temperature difference between the mould section and the molten/solidifying metal ( $\Delta T_1$ ), the heat transfer coefficient ( $h_g$ ) can be calculated using Fourier's law, by first determining the quantity of heat,  $Q$ , flowing through the mould.

$$Q = \frac{kA}{L_2} (\Delta T_2) \quad (1)$$

This is then converted to a heat flux ( $q = \frac{Q}{A}$ ) and then

$$q = h_g (T_{metal} - T_{mould}) = h_g \Delta T_1 \quad (2)$$

is used to determine the heat transfer coefficient,  $h_g$ . In these equations,  $k$  is the thermal conductivity of the mould material and  $A$  is the mould surface area through which heat is transferred.

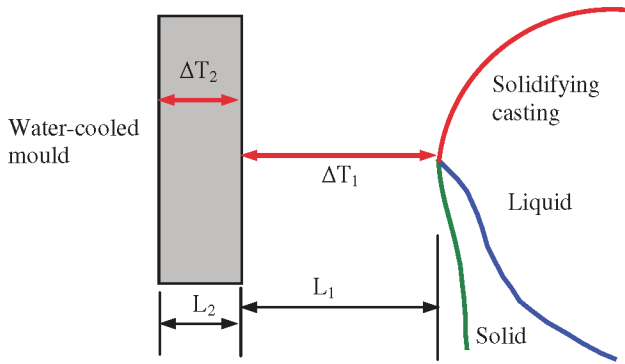


Figure 1. Mould and cast metal configuration showing the essential measurements required to determine the heat transfer coefficient.

In our experimental work, we use these equations to determine  $h_g$  across a fixed (but adjustable) distance  $L_1$  between a molten metal surface and a specially-designed probe that simulates the mould wall. In this way, we determine  $h_g$  as a function of gap distance, and as will be shown later, the gap  $L_1$  has a large influence on  $h_g$ . This feature makes this steady-state experiment unique in that the other experiments reported in the literature only estimate transient values of  $h_g$  [16, 17], whereas our values are for steady-state conditions. The effect of the metal-probe gap on  $h_g$  for the present work is therefore unequivocal.

The method used for the measurement of  $\Delta T_1$ ,  $\Delta T_2$ ,  $L_1$  and  $L_2$  is detailed below. The thermal conductivity,  $k$ , of the mould material is obtained from the relevant literature. The basic experimental arrangement used for the work reported is shown in Figure 2.

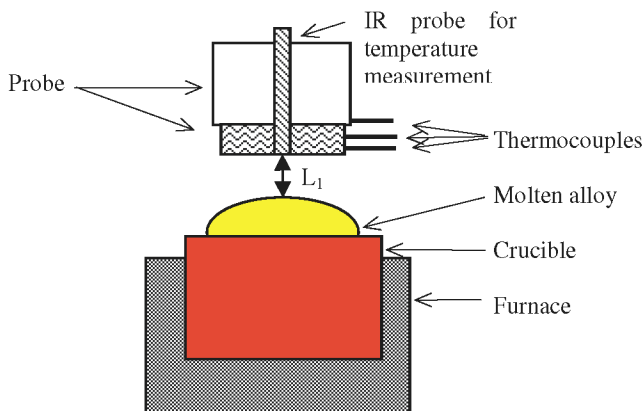


Figure 2. Diagram of the equipment arrangement used for the measurement of heat flow from a hot body to the mould material.

Further details of the probe are shown in Figure 3.

### Equipment design and operation

Whilst the basic concepts described above suggest that the simulation and measurement of the heat flow to the mould wall may be a relatively simple matter, the development of the equipment and methodology for the accurate and repeatable measurement of  $h_g$  involved considerable resources and time. The equipment developed is described by considering the component parts involved for each particular measurement.

#### Data-gathering probe used to simulate the mould

The probe was designed to determine  $\Delta T_2$  (Figure 1). An all metal design was used for the initial work, with a cross section as shown in Figure 3. The probe is mounted in position on a plate capable of precisely-controlled movement in the vertical direction, see Figure 4.  $\Delta T_2$  was determined using 0.25mm diameter, stainless steel sheathed, type K thermocouples embedded into the aluminium probe body (601 alloy<sup>1</sup>) at known positions from the front face of the probe. The distance between the two thermocouples in the bottom of the probe is denoted as  $L_2$  in Figure 1. A third thermocouple was mounted adjacent to the water chamber for the purpose of probe diagnostics.

The major issue was the proper design of the probe to simulate the actual mould as closely as possible. This included, provision of adequate water cooling to prevent heat saturation of the probe during the experiment, and accurate positioning of the thermocouples.

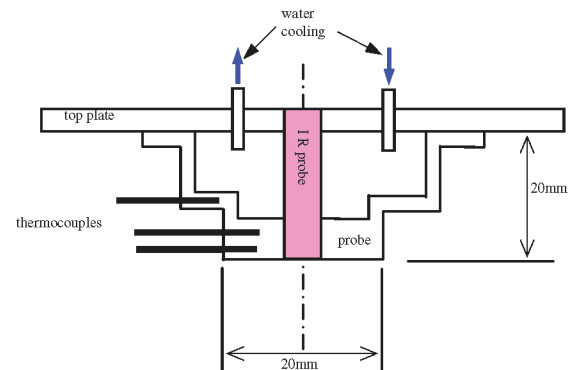


Figure 3. Drawing of the all-metal probe showing the positions of the three thermocouples.

#### Molten metal and $\Delta T_1$

A ceramic crucible, 20mm in diameter and containing ~15 grams of metal was heated by a small resistance furnace with the furnace power, and hence metal temperature, manually controlled. The furnace and crucible were insulated and shielded to prevent stray heat radiation reaching the probe. The temperature of the metal in the crucible was measured using a 2 mm diameter infra-red radiation pyrometer<sup>2</sup> mounted through the centre of the metal probe (Figure 3). A test temperature of  $700 \pm 5$  °C was used. The important issue in this step was to ensure that an essentially flat liquid melt surface faced the probe, since a curved or uneven surface would mean that the gap was not uniform between the

<sup>1</sup> Australian alloy code equivalent to AA356 alloy

<sup>2</sup> Photrix optical thermometer supplied by Lumasence of California, USA.

liquid metal and the probe. The effect of non-uniformity of the gap is explained in the next section.

#### Molten metal/mould gap ( $L_1$ )

The heat transfer coefficient  $h_g$  was found to vary exponentially with the molten metal/mould gap<sup>3</sup> (see Results section). At small gaps, the  $h_g$  value is much higher than at larger gaps. Thus a uniform flat melt surface is critical to define the experimental metal/mould gap. Furthermore, it was important to be able to accurately measure the gap, particularly when small (<1.0mm). A linear voltage displacement transducer (LVDT) calibrated to  $\pm 0.1$ mm was used to measure the gap as it was changed during a test run (Figure 4). The metal/mould gap at the commencement of a test run (zero position for LVDT) was measured using a digital camera with zoom lens together with image analysis software. A further equipment design issue was to protect the LVDT from the crucible heat since the accuracy of the LVDT would be compromised beyond 60 °C.

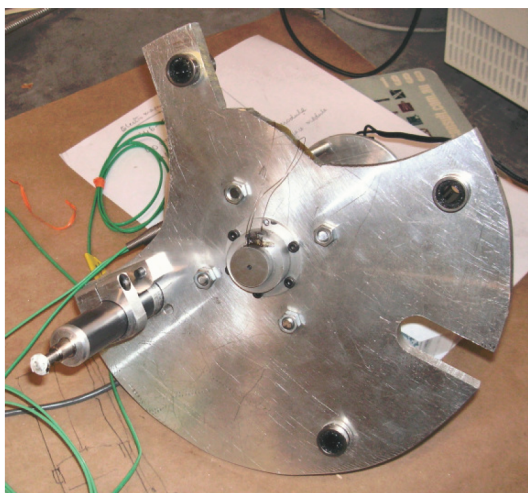


Figure 4. Probe mounting plate with vertical guide bearings. The LVDT is shown mounted underneath together with the all-metal probe. The cut-outs permit access to the furnace area (see Fig. 5).

#### General equipment arrangement

The basic equipment arrangement (shown in Figure 2) was housed in a two part chamber, the general arrangement of which is shown diagrammatically in Figure 5, with the actual apparatus shown in Figure 6.

The two part chamber permitted access to the furnace for: change of alloy; skimming the surface of the molten metal; probe cleaning; and change of mould material including mould insert material. When the chamber was closed it permitted the introduction of various gas species to examine the effect of mould gas flow and composition (the chamber being held at a slight positive pressure from the test gas feed). A specially designed ceramic gas outlet was located adjacent to the probe and at the same height as the front surface (Figure 5). The positions and orientation of the probe and the gas inlet were fixed. Thus while changing the mould-metal gap, the probe and the gas inlet moved

<sup>3</sup> We use metal/mould gap to mean the experimental metal/probe gap in most instances in this paper.

simultaneously. This ensured continuous gas flow between the probe and the melt. The LVDT, thermocouple and gas flow data outputs were connected via a sealed port to a National Instruments data logging system<sup>4</sup> for data recording (one reading every 0.5 seconds) and analysis.

Complementary to the equipment, experimental procedures were developed to ensure that accurate and repeatable results were obtained. Equipment calibration and error checks were incorporated into these procedures, including regular recalibration of the LVDT and the digital camera. The general procedure involved:

1. melting the particular alloy under test;
2. skimming the melt surface;
3. closing the test chamber;
4. introducing the test gas;
5. setting the probe at a starting point (usually 3 – 4 mm from the molten metal surface);
6. recording this point using the digital camera;
7. then, step-wise reducing the molten metal/mould gap until a gap of <0.5mm was reached, while simultaneously recording thermocouple temperatures and LVDT mould gap outputs.

The probe was held at each gap position for approximately 100-150 seconds to ensure that a steady-state heat flow condition was reached. Data processing included checks for thermocouple response, probe heat saturation and reproducibility between duplicate test runs. Results were obtained by two different experimentalists to reduce possible operator bias.

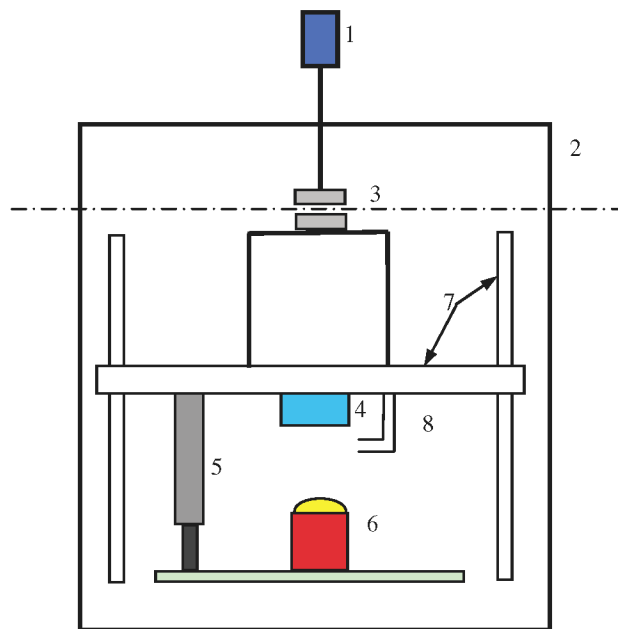


Figure 5. Diagram showing the arrangement of components and the system for varying and measuring the gap between the molten metal and the probe.

The numbered components are:

- 1 - micrometer; 2 - chamber (split into two parts at dashed line); 3 - electro-magnet connecting micrometer system to probe

<sup>4</sup> National Instruments cDAQ 9172 with modules 9211 & 9215

mounting plate; 4 - probe; 5 - LVDT; 6 - furnace and molten sample; 7 - probe mounting plate and guide rails; 8 - gas inlet.



Figure 6. Chamber used for heat flow experimentation. The two sections of the chamber are visible, plus the external actuators, digital camera, and inlets and outlets for various services.

### Results

The heat transfer coefficient between the molten metal and the mould wall in a DC casting mould was found to be dependent upon the size of the gap between the molten metal and the mould wall as shown in Figure 7. The particular set of results shown is for a 601 alloy metal mould (probe body), 99.85% purity aluminium as the molten metal, with a dry air atmosphere. This is a typical result, and the essential shape of the plot remained the same regardless of the test conditions.

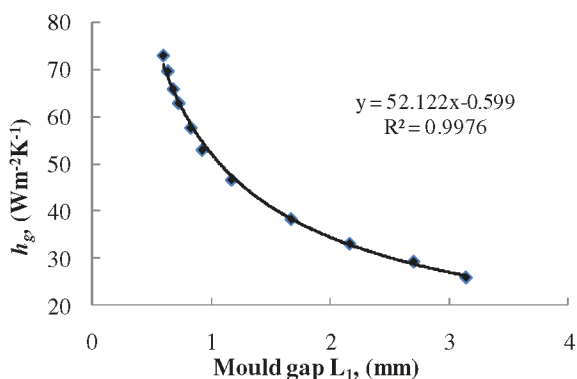


Figure 7. Heat transfer coefficient ( $h_g$ ) versus metal/mould gap size.

The implication of the result shown in Figure 7 is that in the DC casting operation, it is important to take into account that the gap will vary due to meniscus mobility and product shrinkage during solidification. In quoting a value for heat transfer coefficient in the mould wall region it is therefore necessary to quote the  $h_g$  value for a particular gap size. Without this qualification the  $h_g$  value has limited meaning. Even in transient heat flow experiments researchers have found a strong effect of mould-metal gap on the heat transfer coefficient [18]. Furthermore, Trovant and Argyropoulos [19], based on their transient condition

experiments, have concluded that the mould-metal gap formation is the single most important factor governing the heat transfer coefficient.

The results for each particular set of experimental conditions (mould material, molten alloy, mould gas, gas flow, etc.) were plotted and the trend line equations then used to calculate  $h_g$  at a particular mould gap,  $L_1$ . As the inverse relationship ( $h_g$  vs  $1/L_1$ ) is a straight line this was used for the data analysis.

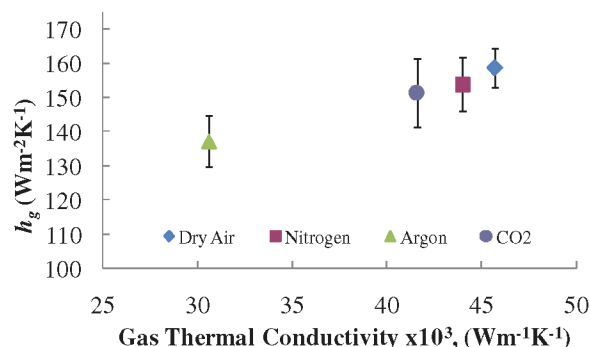


Figure 8. Heat transfer coefficient versus mould gas thermal conductivity for a constant 0.5 mm gap.

The results shown in Figure 8 are for a mould gap of 0.5mm, a value thought to approximate that existing in an operating mould in the region of the molten metal meniscus. Other values may be calculated from the trend line equations, however fixing a particular mould gap permits direct comparison of results obtained under a range of test conditions.

Confidence in the experimental procedures described above was supported by determination of the effect of gas thermal conductivity on  $h_g$  as shown in Figure 8. The results are again for a 601 alloy mould. However, the molten metal used for this set of experiments was replaced by a flat stainless steel cylindrical piece ( $\Phi 20mm$ ) polished to #1200 grit size and heated to 700 °C. The stainless steel piece was used to mitigate the experimental difficulties in maintaining a flat surface with the molten metal. While the actual  $h_g$  values from the stainless steel piece is higher than for aluminium alloys, the  $h_g$  vs. metal/mould gap trend seen in Figure 7 was obtained with the stainless steel experiments as well.

As can be seen from Figure 8, the gas thermal conductivity has a linear effect on the  $h_g$  values. This result supports the present theory that the heat transfer mechanism, between the cast product and the mould wall, is predominately conduction, with radiation and convection probably playing only a small part in the heat transfer process [16]. Helium was also used as a test gas, but the high thermal conductivity of this gas exceeded the capacity of the experimental apparatus to supply sufficient heat to obtain the stable thermal conditions necessary for accurate determination of  $h_g$ . The few data points obtained for Helium did however maintain the linear trend of Figure 8. Such a straight line trend has been predicted by Ho and Pehlke [18] for steady state conditions when the mode of heat transfer is predominantly conduction.



### Discussion and Conclusions

A new technique has been developed to measure the heat transfer coefficient between the metal being cast and the mould within the mould wall region of a DC casting mould. The development of an apparatus and experimental procedures to simulate the metal/mould interaction and determine the heat transfer coefficient has entailed considerable attention to detail together with a large amount of trial and error; mixed with an understanding of the basic science involved, particularly that of heat transfer [20, 21] and of the DC casting process. The challenging issues were: mould gap measurement, particularly when using alloys with a thick oxide; ensuring that the probe only received heat flow from the sample; probe heat saturation; plus the usual issues of thermocouple placement and measurement of thermocouple position.

The example  $h_g$  experimental results shown in Figures 7 & 8 are lower than any previously quoted in the literature (Table 1), although of a similar order to those from References [9, 10]. It is suggested that this is due to the example results being for a precise set of conditions with only one controlled variable (mould gas) and a set mould gap, whereas results generally quoted in the literature account for a range of factors, including different mould materials, alloys, the presence of mould lubricants, etc. and which additionally and most importantly, do not take account of the mould gap effect. In addition, the positions of the thermocouples placed in DC casting moulds and used for mould wall temperature determination are seldom located with the required precision.

The data now being gathered using the apparatus and experimental methods described, permits a detailed and controlled study of the effect of each of the variables that are involved in the transfer of heat from the solidifying casting to a DC casting mould. It may transpire that the actual mould wall heat transfer coefficient is so small in comparison to that of the sub-mould cooling that it may reasonably be neglected, however until this is established and confirmed it is suggested that the possible role of mould wall heat flow in the formation of the cast surface must be seriously considered. It is expected that the present studies using an accurate simulation of the DC casting mould will lead to an improved understanding of the mechanisms involved in the production of high and consistent quality cast product and the control of operating conditions.

As it has long been the aim of DC casters to emulate the conditions of an electromagnetic casting (EMC) mould to produce a product with a smooth, defect free surface with no surface segregation, the results obtained from the present work may assist with this endeavour. It is also suggested that the data may be relevant to more detailed modelling of the DC casting process.

### Acknowledgements

CAST CRC was established under, and is funded in part by the Australian Federal Government's Cooperative Research Centre scheme.

### References

1. J. F. Grandfield et al., "Water Cooling in Direct Chill Casting: Part 2, Effect on Billet Heat Flow and Solidification", *Light Metals*, ed. R. Huglen (TMS, Orlando, Florida, 1997), 1081-1090.

2. J. F. Grandfield, A. Hoadley, and S. Instone, "Water Cooling in Direct Chill Casting: Part 1, Boiling Theory and Control", *Light Metals*, ed. R. Huglen (TMS, Orlando, Florida, 1997), 691-700.

3. H. Yu, "An Experimental Heat Flux Measurement of the Wagstaff Water Hole Mould", *Light Metals*, ed. H. Kvande (TMS, San Francisco, USA, 2005), 983-987.

4. L. Maenner, B. Magnin, and Y. Caratini, "A Comprehensive Approach to Water Cooling in DC Casting", *Light Metals*, ed. R. Huglen (TMS, Orlando, Florida, 1997), 701-708.

5. P. W. Baker, J. F. Grandfield, "Mould Wall Heat Transfer in Air-Assisted DC Casting", *Solidification Processing*, (3rd Conference, The Institute of Metals, London, 1987), 257-260.

6. M. Ekenes, W. S. Peterson, "Visual Observations Inside an Airlip Mould During Casting", *Light Metals*, ed. C. Bickert (TMS, Anaheim, California, 1990), 957 - 961.

7. J. F. Grandfield, and P. T. McGlade, "DC casting of aluminium: Process behaviour and technology", *Materials Forum*, 20 (1996), 29-51.

8. S. Instone, W. Schneider, and M. Langen, "Improved VDC Billet Casting Mould for Al-Sn Alloys", *Light Metals*, ed. P. N. Crepeau (TMS, San Diego, 2003), 725-731.

9. A. Sabau et al., "Heat Transfer Boundary Conditions for the Numerical Simulation of the DC Casting Process", *Light Metals*, ed. A. T. Taberaux (TMS, Charlotte, NC, 2004), 667-672.

10. D. Mortensen, "Mathematical model of the heat and fluid flows in direct-chill casting of aluminum sheet ingots and billets", *Metallurgical Transactions B*, 30B (1999), 119-133.

11. J. M. Drezet et al., "Stress-Strain Computations of the DC Casting Process of Aluminium Alloy: A Sensitivity Study on Material Properties", *Ninth International Conference on Modelling of Casting, Welding and Advanced Solidification Processes*, ed. P. R. Sahm, P. N. Hansen, and J. G. Conley, (Shaker Verlag, Aachen, Germany, 2000), 33-40.

12. K. Ho, "Metal-Mould Interfacial Heat Transfer During the Solidification of Metal Castings", *Engineering Materials*, University of Michigan, Michigan, 1985, 174.

13. M. Trovant, and S. Argyropoulos, "A Technique for the Estimation of Instantaneous Heat Transfer at the Mould/Metal Interface During Casting", *Light Metals*, ed. R. Huglen (TMS, Orlando, Florida, 1997), 927-931.

14. N. Muto, N. Hayashi, T. Uno, Sumitomo Light Metals Technical Reports 37 (1996) 180-184.

15. D. C. Weckman, and P. Niessen, "Numerical simulation of the DC continuous casting process including nucleate boiling heat transfer", *Metallurgical Transactions B*, 13B (1982), 593-602.

16. K. Ho, and R. D. Pehke, "Metal mould interfacial heat transfer", *Metallurgical Transactions B*, 16B (1985), 585-594.

17. M. Trovant, and S. Argyropoulos, "Finding Boundary Conditions: A Coupling Strategy for the Modeling of Metal

Casting Processes: Parts I and II”, *Metallurgical Transactions B*, 31B (2000), 75-96.

18. K. Ho, and R. D. Pehlke, “Transient methods for determination of metal-mould interfacial heat transfer”, *AFS Transactions*, 91 (1983), 689-698.

19. M. Trovant, and S. Argyropoulos, “Finding Boundary Conditions: A Coupling Strategy for the Modeling of Metal Casting Processes: Part I”, *Metallurgical Transactions B*, 31B (2000), 75-86.

20. D. R. Poirier, and E. J. Poirier, *Heat Transfer Fundamentals for Metal Casting* (TMS, USA, 1993), 81.

21. R. H. S. Winterton, *Heat Transfer*, (Oxford University Press, 1997).